(2)

OFFICE OF NAVAL RESEARCH

CONTRACT NO. N0014–89–J–1746

R&T Code 413r001

TECHNICAL REPORT NO. 10

Ultrafast Measurements on Direct Photoinduced Electron Transfer in a Mixed Valence Complex

Gilbert C. Walker, Paul F. Barbara, Stephen K. Doorn, Yuhua Dong and Joseph T. Hupp

Submitted to

Journal of Physical Chemistry

University of Minnesota
Department of Chemistry
Minneapolis, MN 55455

May 6, 1991

Unclassified
SECURITY CLASSIFICATION OF THIS PAGE

REPORT DOCUMENTATION PAGE

Form Approved
OMB No 0704-0188

1a REPORT SECURITY CLASSIFICATION Unclassified	1b RESTRICTIVE MARKINGS
2a SECURITY CLASSIFICATION AUTHORITY	3 DISTRIBUTION / AVAILABILITY OF REPORT Approved for public release distribution unlimited
2b DECLASSIFICATION / DOWNGRADING SCHEDULE	
4 PERFORMING ORGANIZATION REPORT NUMBER(S) Technical Report No. 10	5 MONITORING ORGANIZATION REPORT NUMBER(S)
6a NAME OF PERFORMING ORGANIZATION Department of Chemistry University of Minnesota 6b OFFICE SYMBOL (If applicable)	7a NAME OF MONITORING ORGANIZATION Office of Naval Research
6c ADDRESS (City, State, and ZIP Code) 207 Pleasant St. SE Minneapolis, MN 55455	7b ADDRESS (City, State, and ZIP Code) Chemistry Program 800 North Quincy St. Arlington, VA 2221-
8a NAME OF FUNDING / SPONSORING ORGANIZATION Office of Naval Research 8b OFFICE SYMBOL (If applicable)	9 PROCUREMENT INSTRUMENT IDENTIFICATION NUMBER N0014-89-J-1746
8c ADDRESS (City, State, and ZIP Code) Chemistry Program, 800 N. Quincy St. Arlington, VA 22217	10 SOURCE OF FUNDING NUMBERS PROGRAM ELEMENT NO / PROJECT NO / TASK NO / WORK UNIT ACCESSION NO
11 TITLE (Include Security Classification) Ultrafast Measurements on Direct Photoinduced Electron Transfer in a Mixed Valence Complex	
12 PERSONAL AUTHOR(S) Gilbert C. Walker, Paul F. Barbara, Stephen K. Doorn, Yuhua Dong and Joseph T. Hupp	
13a TYPE OF REPORT Technical 13b TIME COVERED FROM TO	14 DATE OF REPORT (Year, Month, Day) May 6, 1991 15 PAGE COUNT
16 SUPPLEMENTARY NOTATION	
17 COSATI CODES: FIELD / GROUP / SUB-GROUP	18 SUBJECT TERMS (Continue on reverse if necessary and identify by block number)
19 ABSTRACT (Continue on reverse if necessary and identify by block number) See abstract on reverse side	
20 DISTRIBUTION / AVAILABILITY OF ABSTRACT ☒ UNCLASSIFIED/UNLIMITED ☐ SAME AS RPT ☐ DTIC USERS	21 ABSTRACT SECURITY CLASSIFICATION Unclassified
22a NAME OF RESPONSIBLE INDIVIDUAL Dr. Ronald A. De Marco	22b TELEPHONE (Include Area Code) / 22c OFFICE SYMBOL

DD Form 1473, JUN 86 Previous editions are obsolete.

S/N 0102-LF-014-6603

SECURITY CLASSIFICATION OF THIS PAGE
Unclassified

19.

Abstract

A direct measurement of the kinetics of intramolecular photoinduced metal–metal–charge transfer has been made, i.e.

$$(NH_3)_5Ru^{III}NCFe^{II}(CN)_5^- \underset{k_{et}}{\overset{h\nu}{\rightleftharpoons}} (NH_3)_5Ru^{II}NCFe^{III}(CN)_5^-$$

where the solvent is H_2O or D_2O and k_{et} signifies the the reverse electron transfer (et) rate coefficient. The apparent reverse electron transfer kinetics are non–exponential with a limiting rate constant, $k_{lim} = \lim_{t\to\infty} k(t)$, equal to $8\pm3 \times 10^{11} sec^{-1}$. This is close to the theoretical predictions from the model of Sumi and Marcus (classical vibrational modes) $k_{et,SM} = 10^{13}$ and 5×10^{12} sec^{-1}, and from the model of Jortner and Bixon (quantum mechanical vibrations) $k_{et,JB} = 1.2\times10^{12} sec^{-1}$. The parameters required for these theories have estimated by resonance Raman spectroscopy and other means.

J. Phys. Chem.

submitted.

Ultrafast Measurements on Direct Photoinduced Electron Transfer in a Mixed Valence Complex

Gilbert C. Walker, and Paul F. Barbara*

Department of Chemistry, University of Minnesota, Minneapolis, MN 55455

Stephen K. Doorn, Yuhua Dong, and Joseph T. Hupp

Department of Chemistry, Northwestern University, Evanston, IL

---

* Author to whom correspondence should be addressed

Abstract

A direct measurement of the kinetics of intramolecular photoinduced metal–metal–charge transfer has been made, i.e.

$$(NH_3)_5Ru^{III}NCFe^{II}(CN)_5^- \underset{k_{et}}{\overset{h\nu}{\rightleftharpoons}} (NH_3)_5Ru^{II}NCFe^{III}(CN)_5^-$$

where the solvent is H_2O or D_2O and k_{et} signifies the the reverse electron transfer (et) rate coefficient. The apparent reverse electron transfer kinetics are non–exponential with a limiting rate constant, $k_{lim} = \lim_{t\to\infty} k(t)$, equal to $8\pm3 \times 10^{11} sec^{-1}$. This is close to the theoretical predictions from the model of Sumi and Marcus (classical vibrational modes) $k_{et,SM} = 10^{13}$ and 5×10^{12} sec^{-1}, and from the model of Jortner and Bixon (quantum mechanical vibrations) $k_{et,JB} = 1.2\times10^{12} sec^{-1}$. The parameters required for these theories have estimated by resonance Raman spectroscopy and other means.

INTRODUCTION

Compounds exhibiting mixed valence metal–metal charge transfer transitions MMCT)[1] have played a central role in the development of the understanding of electron transfer (et) reactions. In Marcus' theory of et[2], the energy of the absorption maximum $h\nu_{max}$ gives direct information on the reorganization energy λ, as follows

$$h\nu_{max} = \lambda + \Delta G^{O} \qquad (1)$$

where h is Plank's constant and ΔG^{O} is the driving force, as shown in Figure 1, which represents the reaction described in this paper.

The MMCT absorption band also gives a measure of a key et parameter, the electronic matrix element V_{el}.[3] Resonance Raman spectroscopy on the MMCT band gives detailed information on the vibrational modes that are coupled to the et reaction.[4] Two additional types of data are needed for an "absolute" rate prediction, namely, a measure of the dynamics of the solvent coordinate and a measure of the reaction driving force, ΔG^{O}. For a typical MMCT compound, such as in Figure 1, ΔG^{O} can be approximately estimated from redox potentials of the isolated metal systems or other methods. Estimates for the required solvation dynamical information is available from recent transient Stokes–shift measurements on polar fluorescent probes.[5] In summary, all the required parameters that are necessary to make a prediction of the et rate constant, k_{et}, for MMCT compounds can be experimentally obtained, but no such comparison has been reported to our knowledge.

In this paper, we report the first direct kinetic measurement of a MMCT optically induced et reaction, as represented in Figure 1, and compare the experimental results to theoretical predictions using experimentally estimated parameters. It should be noted that a report has appeared in which MMCT kinetics were indirectly induced by metal–ligand–charge–transfer optical excitation.[6] Our work is oriented, in part, toward evaluating contemporary theoretical models that explicitly consider the dramatic effect of solvation dynamics on et rates.[7] In the last decade it has been established that et rates can be directly proportional to the time scale for solvent motion for simple systems in certain

limits,

$$k_{et} \simeq \tau_s^{-1} \exp(-\Delta G/k_b T) \qquad (2)$$

and thus for small barrier reactions ($\Delta G << k_b T$) k_{et} is solvent controlled, i.e. $k_{et} \simeq \tau_s^{-1}$. We are particularly concerned in this paper with obtaining experimental evidence on how the simple picture of eqn. 2 is affected by strong electronic coupling, vibrational modes, and frequency dependent solvent friction effects.[7]

Experimental Methods

The transient pump–probe apparatus has been described elsewhere.[8] The laser source is an intermediate repetition rate (8.2kHz) amplified dye laser (λ=792nm) with 70fs pulse duration. The energy of the pump and probe pulses were typically 400 and 20 nJ, respectively. The spot sizes were $\simeq$100μm. The continuum light probe pulses were generated in water or a mixture of water and ethylene glycol. The general synthetic procedure of Voger and Kisslinger[9] was used to prepare $(NH_3)_5Ru^{III}NCFe^{II}(CN)_5^-$, except that samples were further purified by passage through a DOWEX 50WX8 cation exchange column. Sample concentrations were typically $5x10^{-3}$ molar.

Results and Discussion:

Static Spectroscopy

We have recorded transient pump–probe spectroscopy of the MMCT transition of $(NH_3)_5Ru^{III}NCFe^{II}(CN)_5^-$, as shown in Figure 1.

The MMCT band of RuFe in water is peaked at 10,200cm^{-1} (975nm) and has a bandwidth of 4900cm^{-1}. It is not overlapped by any other observable optical transition of RuFe. The molar extinction coefficient of the MMCT band, ϵ_{max} = 3000cm^{-1}, and the bandwidth can be used to estimate the electronic matrix element V_{el}.[3,10] The estimated value (1500cm^{-1})[10] is large and is indicative of a relatively strong metal–metal interaction due to the short metal–metal distance and the interaction provided by the cyanide bridging

ligand.

The maximum energy of the absorption maximum, $h\nu_{max}$, gives an estimate of the total reorganization energy.

$$\lambda \equiv h\nu_{max} - \Delta G^{o} \cong \lambda_{class} + \lambda_{QM} \qquad (3)$$

where λ_{class} and λ_{QM} are the low frequency (classical) and high frequency (quantum mechanical) contributions to the total reorganization energy and ΔG^{o} is the driving force of the et. Eqn. 3 is an approximation, although it is valid when the solvent broadening is strong enough to ensure a structureless band, see Kjear and Ulstrup.[12]

We have collected resonance Raman data on RuFe and analyzed it within the harmonic approximation to yield the coordinate displacements and the vibrational fundamental frequencies[13] as shown in Table 1. From the displacements and frequencies, a reorganization energy λ_i for each ith mode can be estimated. The total vibrational reorganization energy is $\lambda_{vib} = \Sigma\lambda_i \simeq 3200 cm^{-1}$. The solvent reorganization energy can be estimated to be $\lambda_{solv} \simeq 2400 cm^{-1}$ (see ref. 12 for more details). λ_{vib} is identified with λ_{QM}, and λ_{solv} is assumed to be the dominant contribution to λ_{class}, i.e. $\lambda_{class} \simeq \lambda_{solv}$. In a later section we consider an alternative approximation for the decomposition of λ into λ_{solv} and λ_{vib}.

Ultrafast pump–probe spectroscopy

Figure 2a shows a pump–probe, optical density transient for $Ru^{III}Fe^{II}$ in H_2O at $293^{o}K$, where $\lambda_{pump} = \lambda_{probe} = 792nm$. The upward direction in Figure 2 corresponds to a negative optical density, i.e. decreasing absorption or "bleach". The optical transient can be fit well by a convolution of a triexponential model decay $OD(t) = A_1 \exp(-t/\tau_1) + A_2 \exp(-t/\tau_2) + A_3 \exp(-t/\tau_3)$ and the experimental instrument response function. A typical set of parameters is as follows (with the amplitudes represented as percentages) $\tau_1 = 0.05ps(86\%)$, $\tau_2 = 1.2ps(12\%)$, $\tau_3 > 75ps(1.5\%)$. These parameters are not significantly dependent on laser power (varied by a factor of 5), relative

polarization of the pump and probe pulses, and the concentration of $Ru^{III}Fe^{II}$ (varied over a factor of 10). For the purpose of discussion we denote the three kinetic components as processes I,II,and III, in order of decreasing rate.

We have also detected the transient pump–probe signal (λ_{pump}=792nm) with λ_{probe}=820nm (Fig. 3a) and, alternatively, λ_{probe}=700nm (Fig. 3b). The signal–to–noise of these latter two transients is much less than the experiments in Figure 2 because the probe light for Figure 3 was continuum and has more intensity fluctuation than the 792nm laser source which was used in in the experiments in Figure 2. Nevertheless, the dynamics we observe at λ_{probe}=792nm are qualitatively similar to the dynamics at λ_{probe}=820nm and λ_{probe}=700nm within the marginal signal to noise of the measurements of Figure 3. However, the pulse limited ($\tau\simeq$50fs) component component I has a (abt 2x) smaller relative amplitude in the measurements with $\lambda_{pump} \neq \lambda_{probe}$, suggesting that component I is partly due to a coherent artifact.[14] However, the fact that component I is still observed when the probe wavelength is extensively detuned from the pump wavelength (Fig. 3b) suggests that some of component I may be due to an ultrafast component of k_{et}.

The interpretation of component II is more straightforward because coherent artifacts are an unlikely complication at this time scale ($\tau\simeq$1ps vs $\simeq$0.1ps pulse width). We tentatively assign component II to direct, ground state recovery, i.e. et, although more extensive, variable wavelength pump–probe measurements are in progress to evaluate this assignment. The slowest kinetic process (component III) is assigned to an unresolvably slow decay of a small fraction (<10%) of the excited molecules due to an unassigned side reaction , such as from $Ru^{II}Fe^{III}$ to another excited electronic state of $Ru^{III}Fe^{II}$, which would subsequently relax (perhaps slowly) to ground state $Ru^{III}Fe^{II}$.

We have also measured the pump–probe signal in D_2O instead of H_2O, see Fig. 2b. There is a clear diminution in the rate of absorption recovery. We note that when $Ru^{III}Fe^{II}$ is dissolved in D_2O ammine protons may exchange with solvent deuterons. Further experiments are underway to examine the consequences of this exchange.

In conclusion, pump–probe measurements on the MMCT band of $Ru^{III}Fe^{II}$ show three apparent time scales for absorption recovery. The second component (τ_2=1.2ps) has been assigned to direct et ($Ru^{II}Fe^{III} \rightarrow Ru^{III}Fe^{II}$), while the fastest process may be due partly to et and partly to a coherent artifact. The experimental measurements, therefore, indicate that the rate of direct photo–induced et falls in the range 10^{13}–10^{12} sec^{-1}, depending on whether component I is partly due to et.

Theoretical Predictions

Contemporary et theory involves an explicit treatment of the recently recognized, important role of solvation dynamics in et kinetics.[7,15-19] It is convenient to consider two specific theoretical models which treat the interplay of solvation dynamics and vibrational degrees of freedom, namely: the theory of Sumi and Marcus[16a], which treats the vibrational modes classically, and the theory of Jortner and Bixon[17] that involves a quantum mechanical model for the vibrations.

Both of these models involve a simple "Debye" model for the dynamics of the solvent coordinate involving a single relaxation time. Simulations on the self–exchange et of Fe^{II}/Fe^{III} by Bader *et al.*[18] and related simulations in water[7] indicate that more complex solvation dynamics actually exist in aqueous environments. The impact of the complex solvation dynamics has been discussed by Hynes *et al.*[12] and others[7], in terms of a frequency dependent solvent friction formulation.

The theoretical treatment of Sumi/Marcus[16a] is based on a diffusive mechanism for the solvent coordinate. The actual et event is assumed to occur along vibrational coordinates which are treated classically. A key element is the solvent coordinate dependent rate coefficient,

$$k(x) = \nu_q \exp(-\Delta G^*(x)/k_b T) \qquad (4)$$

where ν_q is the effective frequency factor and $\Delta G^*(x)$ is the x dependent activation energy. For the reaction $Ru^{II}Fe^{III} \rightarrow Ru^{III}Fe^{II}$, V_{el} is large enough to ensure that the adiabatic

expression for ν_q is appropriate, as follows

$$\nu_q = (\Sigma_j \nu_j^2 \lambda_j / \lambda_{vib})^{1/2} \simeq 1200 cm^{-1} \qquad (5)$$

where λ_{vib} is the total vibrational reorganization energy and the values in Table 1 have been used in eqn (5). The remaining necessary parameters are the solvent reorganization energy λ_{solv}, the driving force, and the solvent relaxation time τ_s, which are listed in Table 2.

Employing these parameters, the Sumi/Marcus prediction for the rate, k_{SM} (see Table 2), is obtained by use of the numerical results in Figures 2 and 3 of reference 16a. k_{SM} is multi–exponential, reflecting (1) a rapid et that occurs from an already favorable solvent distribution and (2) a slower et influenced by solvent diffusion.

In contrast to the Sumi/Marcus model, the Jortner/Bixon[17] approach treats the vibrational coordinates quantum mechanically. In particular, a single vibrational mode is employed, and the total et rate from v=0 of the reactant to all possible vibrational levels n of the product is given by

$$k_{et} = \sum_n k_{NA}^{0n} / (1 + \mathcal{H}_A^{(n)}) \qquad (3)$$

where n refers to the quantum level of the high frequency accepting mode in the product state. k_{NA}^{0n} is the nonadiabatic rate constant for each vibronic channel, i.e.

$$k_{NA}^{0n} = \frac{2\pi V^2}{\hbar (4\pi\lambda_{solv} k_B T)^{\frac{1}{2}}} \exp(-\Delta G_{on}^{\ddagger} / k_b T) \qquad (4)$$

where V_n is the Frank–Condon "dressed" matrix element and $\Delta G_{on}^{\ddagger}$ is the effective activation energy for the 0→n channel. The adiabicity parameter $\mathcal{H}_A$ in eqn 3 is given as $\mathcal{H}_A = 4\pi V_n^2 \tau_s / h\lambda_{solv}$, where we have substituted τ_s, the experimentally measured solvation time, for τ_l, th continuum estimate for the solvation time which was used by Jortner and Bixon.

The Jortner/Bixon model employs a single effective vibrational degree of freedom. In order to invoke this theory we use the average vibration frequency estimated by eqn 5 and the reorganization energy in that "average" mode to estimate the Frank–Condon

factors.[13,17] The Jortner/Bixon rate k_{JB} employing this effective vibrational mode is given in Table 2, and the Jortner/Bixon rate is dominated by the third vibronic channel, 0–2, which is predicted to be solvent controlled.

The Sumi–Marcus analysis, which includes all reorganization energy in calculating ΔG^*, results in a "normal regime", nearly "barrierless regime" et. Due to the magnitude of ΔG^o, the partitioning of vibrational reorganization energy into quantal degrees of freedom results in the Jortner/Bixon "inverted regime" prediction, which then depends quantal degrees of freedom to reduce the effective activation barrier to enhance k_{et}.

Comparison of Theory and Experiment and Frequency Dependent Solvent Friction

It is noteworthy that the experimental results agree with both theoretical results to within a factor of roughly 4, generally supporting the validity of these models. Both models point out the importance of the vibrational coordinates, though in surprisingly different ways. In the Sumi/Marcus case, vibrational frequencies enter most significantly in the preexponential factor, ν_q. In the Jortner/Bixon case, quantal vibrations serve to reduce the effective activation barrier. However, the enhancement of k_{JB} due to quantal effects is not as large as the 10^5 "quantal" enhancement recently observed in the "inverted regime" et of betaine–26[8a].

Both theoretical models predict that the et rate is diminished by dynamic solvent effects. Indeed, the predicted rate according to the Jortner/Bixon model is close to $1/\tau_s$ which implies that the et kinetics may depend on the initial distribution along the reaction coordinate. Since the et reaction in this paper is initiated by ultrafast laser excitation, the solvent coordinate is actually prepared in a displaced configuration, rather than the equilibrated configuration in $Ru^{II}Fe^{III}$ which is more consistent with the theoretical models. Nevertheless, the Jortner/Bixon prediction that $k_{et} \simeq \tau_s^{-1}$ should still apply even though solvent diffusion is occurring from the "high energy side" of the avoided crossing, see Figure 1.

It should be emphasized that the Sumi/Marcus and Jortner/Bixon predictions made above are based on the assumption that the solvent coordinate relaxation is overdamped and is manifested by a single relaxation time. However, molecular dynamics simulations of solvation of Fe^{II}/Fe^{III} in water[18], and related simulations of solvation in water[7], reveal a complex dynamical behavior indicative of inertial motion at early times (<50fs) involving librations of water and diffusional motion at later times. Although the transient Stokes shift measurements on polar fluorescent probes in water measured a distribution of solvation components (or frequency dependent solvent friction)[7], the initial, faster components are apparently too rapid to resolve by existing transient emission methods.[8]

Hynes and co–worker[19] have shown that frequency dependent solvent friction can dramatically alter theoretical predictions of k_{et}. In order to estimate roughly the role of frequency dependent solvent friction in the case of $Ru^{II}Fe^{III}$ we have separated the solvent coordinate into a low frequency (lf) and high frequency (hf) contribution which we model classically and quantum mechanically, respectively. The parameters are as follows: $\lambda^{(lf)}_{solv,cl}$ = 1600cm^{-1}, $\lambda^{(hf)}_{solv,qm}$ = 800cm^{-1}, and $\nu^{(hf)}_{solv,qm}$ = 400cm^{-1}, which have been roughly estimated from the power spectrum of the solvation dynamics of the bulk solvent in Chandler and co–worker's[18] simulation of solvation dynamics of aqueous Fe^{II}/Fe^{III}. Our treatment thus includes two quantum modes (one intramolecular and one solvent) and one classical bath.

The Jortner/Bixon prediction using this modified treatment of the solvent is denoted by $k_{JB,mod}$ in Table 2. Note that this result is faster than k_{JB} because the effective solvent barrier has been reduced by partitioning some of the solvent reorganization energy to a quantal mode and allowing combination $(V_1,V_2) \rightarrow (V'_1V'_2)$ vibronic transitions.

Acknowledgements

PFB would like to acknowledge the National Science Foundation, and Office of Naval Research for partial support of this research. JTH acknowledges support from the

U.S. Department of Energy, Office of Energy Research, Division of Chemical Sciences (Grant No. DE–FGO2–87ER13808) and the Alfred P. Sloan Foundation.

REFERENCES

1. Creutz, C. *Prog. Inorg. Chem.* **1983**, *30*, 1.

2. Marcus, R.A. *Ann. Rev. Phys. Chem.* **1964**, *15*, 155. Marcus, R.A.; Sutin, N. *Biochem Phys. Acta* **1985**, *811*, 265.

3. Hush, N.S. *Prog. Inorg. Chem.* **1967**, *8*, 391.

4. Doorn, S.K.; Hupp, J.T., *J. Am. Chem. Soc.*, **1990**, *112*, 4999. Doorn, S.K.; Hupp, J.T. *J. Am. Chem. Soc.* Soc., **1990**, *111*, 1142.

5. Jarzeba, W.; Walker, G.C.; Johnson, A.J.; Kahlow, M.A.; Barbara, P.F. *J. Phys. Chem.* **1988**, *92*, 7039. Walker, G.C.; Jarzeba, W.: Johnson, A.E.; Barbara, P.F., *manuscript in preparation.*

6. Creutz, C.; Krofer, P.; Matsubara, T.; Netzel, T.L.; Sutin, N. *J. Am. Chem. Soc.* 1979. *101*, 5442.

7. For recent reviews on dynamic solvent effects on et kinetics, see Barbara, P.F.; Jarzeba, W. *Adv. Photochem.* **1990**, *15*, 1. Maroncelli, M.; MacInnis., J.; Fleming, G.R. *Science* **1989**, *243*, 1674. Simon, J.D. *Acc. Chem. Res.* **1988**, *21*, 128. Weaver, M.J.; McManis III. G.E. *Acc. Chem. Res.* **1990**, *34*, 294.

8. Åkesson, E.; Walker, G.C.; Barbara, P.F. *J. Chem. Phys.*, submitted. Kahlow, M.J.; Jarzeba, W.; DuBruil, T.P.; Barbara, P.F. *Rev. Sci. Inst.* **1988**, *59*, 1098.

9. Vogler, A; Kisslinger, J. *J. Am. Chem. Soc.* **1982**, *104*, 2311.

10. Burewicz, A. Haim, A. *Inorg. Chem.* **1988**, *27*, 1611.

11. To avoid using eletrochemical estimates of the driving force which include considerable approximations, we have estimated the driving force as follows. We first estimate λ_{solv} using the Marcus[2] expression, $\lambda_{solv,theo} = e^2(1/2r_1 + 1/2r_2 + 1/d)(1/D_{op} - 1/D_{static})$, where e is the charge transfered, r_1=4.4Å, r_2=3.5Å, d=5.1Å, and the Peckar factor is 0.55. Then, recognizing that this expression may overestimate λ_{solv}, we assume that $\lambda_{solv} \simeq 0.6\ \lambda_{solv,theo}$ based on estimates from several better characterized systems, see for instance Hupp, J.T.; Meyer, T.J. *Inorg. Chem.* **1987**, *26*, 2332. Creutz, C. *Inorg. Chem.* **1978**, *17*, 3723. Oh, D.; Boxer, S.G. *J. Am. Chem. Soc.* **1989**, *111*, 1130. Using r_1 = 4.4Å(, r_2 = 3.5Å, and d = 5.1Å we obtain $\lambda_{solv,theo} \simeq 3800cm^{-1}$. Thus $\lambda_{solv} \simeq 2400cm^{-1}$. This results in $\Delta G^0 \simeq 4600cm^{-1}$. An alternative technique uses the electrochemical data[10] of the individual metal complexes to predict a driving force of $\simeq 3000cm^{-1}$. Then using this value, λ_{vib} from the resonance Raman data, and $h\nu_{abs,max}$ one can then estimate λ_{solv} as $4900cm^{-1}$. Incorporating the values from the electrochemically based calculation in a theoretical analysis analagous to that summarized in Table 2, the Sumi–Marcus rate

becomes single exponential, with $k_{et,SM} \simeq 4.4 \times 10^{11} sec^{-1}$. The Jortner/Bixon rate is nearly unchanged, $k_{et,JB} \simeq 1.0 \times 10^{12} sec^{-1}$. In this case, the Jortner/Bixon et is a "normal regime" et, and the similarity of the two Jortner/Bixon predicted rates results from several favorable Frank–Condon factors.

12. Kjear, A.M.; Ulstrup, J. *J. Am. Chem. Soc.* **1987**, *109*, 1934.

13. Heller, E.J. *Acc. Chem. Res.* **1981**, *14*, 368. Tannor, D.; Heller, E. *J. Phys. Chem.* **1982**, *77*, 202. Heller, E. J; Sundberg, R. L.; Tannor, D. *J. Phys. Chem.* **1982**, *86*. 1822.

14. von Jena, A.; Lessing, H.E. *Appl. Phys.* **1979**, *19*, 131.

15. Huang, J–K.; Creighton, S.; King, G.; Whitney, D. Warshel, A. *J. Chem. Phys.*, in press. Warshel, A. Chu, Z.T. *J. Chem. Phys.* **1990**, *93*, 4003.

16. (a) Sumi, H.; Marcus, R.A. *J. Chem. Phys.* **1986**, *84*, 4894; (b) Nadler, W.; Marcus. R.A. *J. Chem. Phys.* **1987**, *86*, 3906.

17. Jortner, J.; Bixon,M. *J. Chem. Phys.* **1988**, *88*, 167.

18. Bader, J.S.; Chandler, D . *Chem. Phys. Lett.* **1989**, *157*, 501. Bader, J.S.; Kuharski, R.A.; Chandler, D . *J. Chem. Phys.* **1990**, *93*, 230.

19. van der Zwan, G.; Hynes, J.T. *J. Phys. Chem.* 1985, *89*, 4181. Hynes, J.T. *J. Phys. Chem.* **1986**, *90*, 3701. Ciccotti, G.; Ferrario, M.; Hynes, J.T.; Kapral, R. *J. Chem. Phys.* **1990**, *93*, 7137.

20. $k_{JB,mod}$ exceeds $1/\langle \tau_s \rangle$. This result, however, may be unphysical because k_{et} should not significantly exceed the rate of diffusion ($K_D \simeq \tau_s^{-1} \simeq 2 \times 10^{12} sec^{-1}$) from the bottom of the well to the lowest energy avoided crossing (0→0). Apparently the generalized Jortner/Bixon model overestimates the total rate because it simply adds partial rates of individual channels, which is not physically correct since the various adiabatic channels should effectively "kinetically interfere". Instead a more fundamental theoretical approach is required. However, such an approach is computationally intensive and beyond the scope of this paper.

Table 1. Structural and Frank–Condon Charge Transfer Parameters for $(NH_3)_5Ru–NC–Fe(CN)_5^-$ from Postresonance Raman ($\lambda_{exc.}$ = 647.1nm)

Band(cm^{-1})	Assignment	$I_{rel}^{a,b}$	$\lvert\Delta a\rvert$(Å)^{b,c,d}	$\lambda_1'(cm^{-1})^{b,c,d,e}$
2104	$\nu_{C\,N,\ bridge}$	15	0.045	870
2060	$\nu_{C\,N,\ term.}$	1.3	0.0069	80
603	$\nu_{Fe–C,\ bridge}$	4.1	0.039	830
544	$\nu_{Fe–C,\ term.}$	0.92	0.043	210
482	$\nu_{Ru–NH_3}$	1.0	0.034	250
468	$\nu_{Ru–NH_{3,axial}}$	0.53	0.052	140
361	$\nu_{Ru–NC}$	0.34	0.049	120
270	$\delta_{H_3N–Ru–NH_3}$	1.6	–	720

[a] Relative Raman scattering intensity; all modes are resonantly enhanced.

[b] Raman data were obtained at postresonance. Detailed spectral simulations suggest that some minor re–ordering of relative scattering intensities (and therefore $\lvert\Delta a\rvert$ and λ_{vib}' values) will be observed when experiments are performed at preresonance. The simulations also suggest that the most accurate structural parameters will be obtained at preresonance.

[c] A description for the derivation of these values may be found in reference 4. The value of σ used in this calculation was 1740cm^{-1}. Solvent reorganization was assumed not to contribute to the overall breadth of the absorption band, adding breadth instead only to the individual vibrational components

[d] Absolute bond length displacements following electron transfer; derived values are based on a local mode approximation (see ref. 4.)

[e] Single mode contribution to the total vibrational reorganization energy.

Table 2. Predicted Electron Transfer Rates for $Ru^{II}Fe^{III} \rightarrow Ru^{III}Fe^{II}$, with associated parameters[a]

theory	k_{et}	λ_{class}	λ_{sol}	$\lambda_{class,vib}$	λ_{QM}	ν_{QM}	$\frac{1}{<\tau_s>}$
Sumi/Marcus	10 & 5[b]	5600	2400	3200	–	[c]	1.7
Jortner/Bixon	1.2	2400	2400	–	3200	1225	1.7
Sumi/Marcus (modified)	1.1 & 0.8[b]	3200	2400	800	–	[d]	1.7
Jortner/Bixon (modified)	8.0	1600	1600	–		[e]	1.7

[a] All rates are in units of $10^{12}sec^{-1}$. Reorganization energies λ are in units of cm^{-1}. The driving force $\Delta G^{o} = 4600cm^{-1}$.

[b] Two characteristic rates result from this analysis, see text for further details.

[c] The average phonon frequency ν enters into the Sumi–Marcus expression (eqn 4.6 in ref. 16a) which is used as part of estimating k_{et}, i.e. $\nu = \nu_{q}(\lambda_{class,vib}/\lambda_{class})^{1/2} = 2.9x10^{13}sec^{-1}$.

[d] As in [c], except $\nu = 3.4x10^{13}\ sec^{-1}$

[e] In this analysis there are two quantum modes, one intramolecular and one solvent. Their frequencies and reorganization energies are $\nu_{qm} = 1225\ cm^{-1}$ (λ_{qm}=3200cm^{-1}) and $\nu_{qm,solv} = 400cm^{-1}$ ($\lambda_{qm,solv}$=800cm^{-1}), respectively. See text for further details.

Figure 1. $Ru^{III}Fe^{II}$ (left) and $Ru^{II}Fe^{III}$ (right) free energy surfaces generated using a classical model for all of the reorganization energy. In a schematic description, the pump laser (792nm) induces direct, optical electron transfer (the vertical arrow) and the reverse electron transfer rate (which might occur as schematically shown by the downward arrows) is measured by optically probing the recovery of the initial population.

Figure 2. (a) The transient bleach signal of $(NH_3)_5Ru^{III}NCFe^{II}(CN)_5^-$ in H_2O with pump and probe at 792nm. The sharp peak at early time is the instrument response function (offset for visual clarity). The data (circles) is fit with the asymmetric curve which corresponds to a convolution of the instrument response function and three exponential model for the decay. The fitted values are τ_1=0.05psec(86%), τ_2=1.2psec(12%), and τ_3>75psec(1.5%). We assign the second component to reverse electron transfer, although some of the faster component may also reflect reverse electron transfer (see text for details). (b) A comparison of the transient signal in H_2O (lower trace) and D_2O (upper trace).

Figure 3. Pump–probe transients of $Ru^{III}Fe^{II}$ in H_2O where the probe light comes from selecting a wavelength fraction of white light continuum. Upper figure is 792nm pump and 700nm probe. Lower figure is 792nm pump and 820nm probe. The two color transients show qualitatively the same features as the one color measurements (fig. 2) although the amplitude off the fastest component appears to be smaller in the two color measurements suggesting that coherent effects probably contributed to the fast component observed in the one color measurement (see text).

FIGURE 1

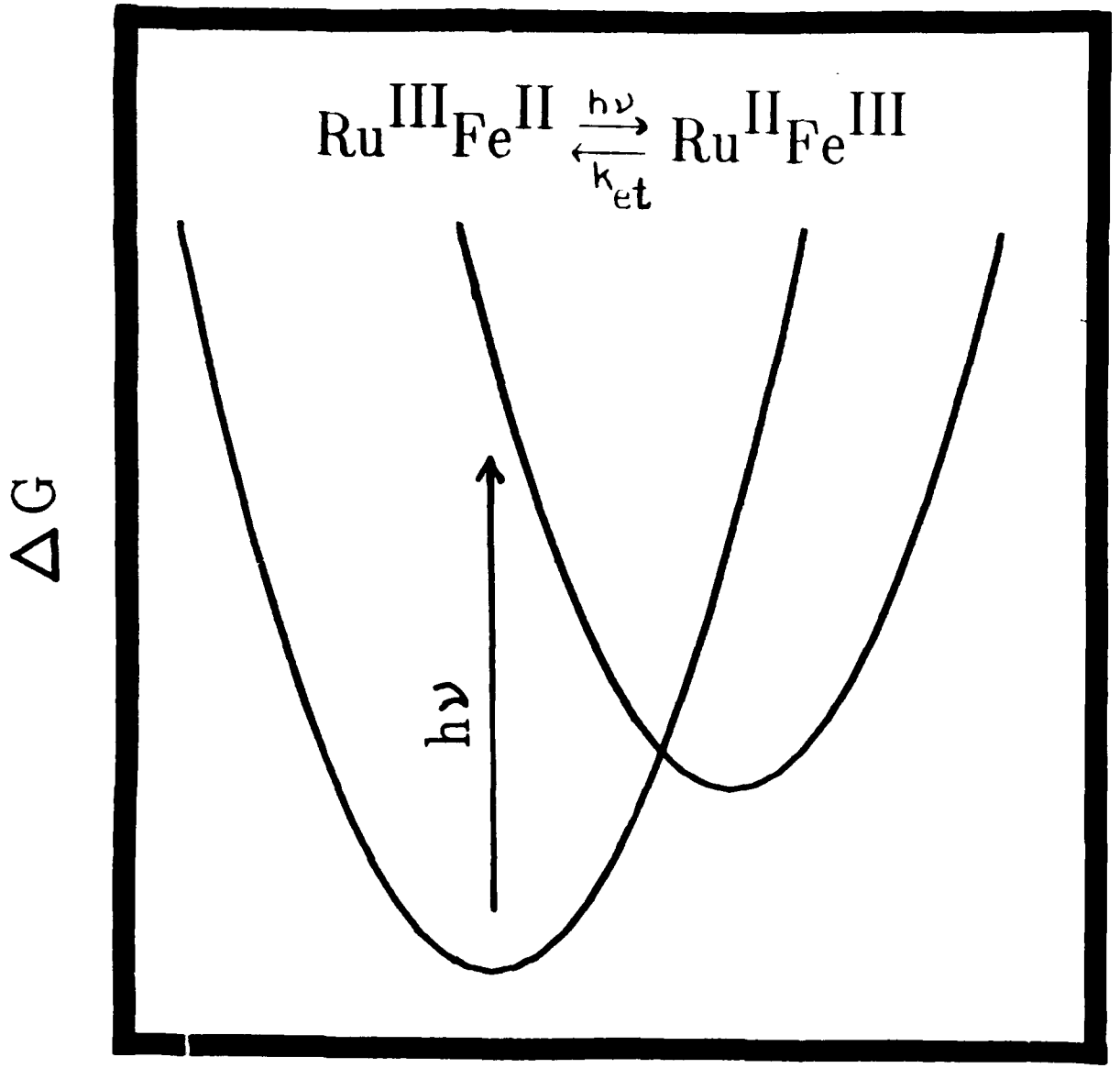

solvent polarization and ligand motion

FIGURE 2

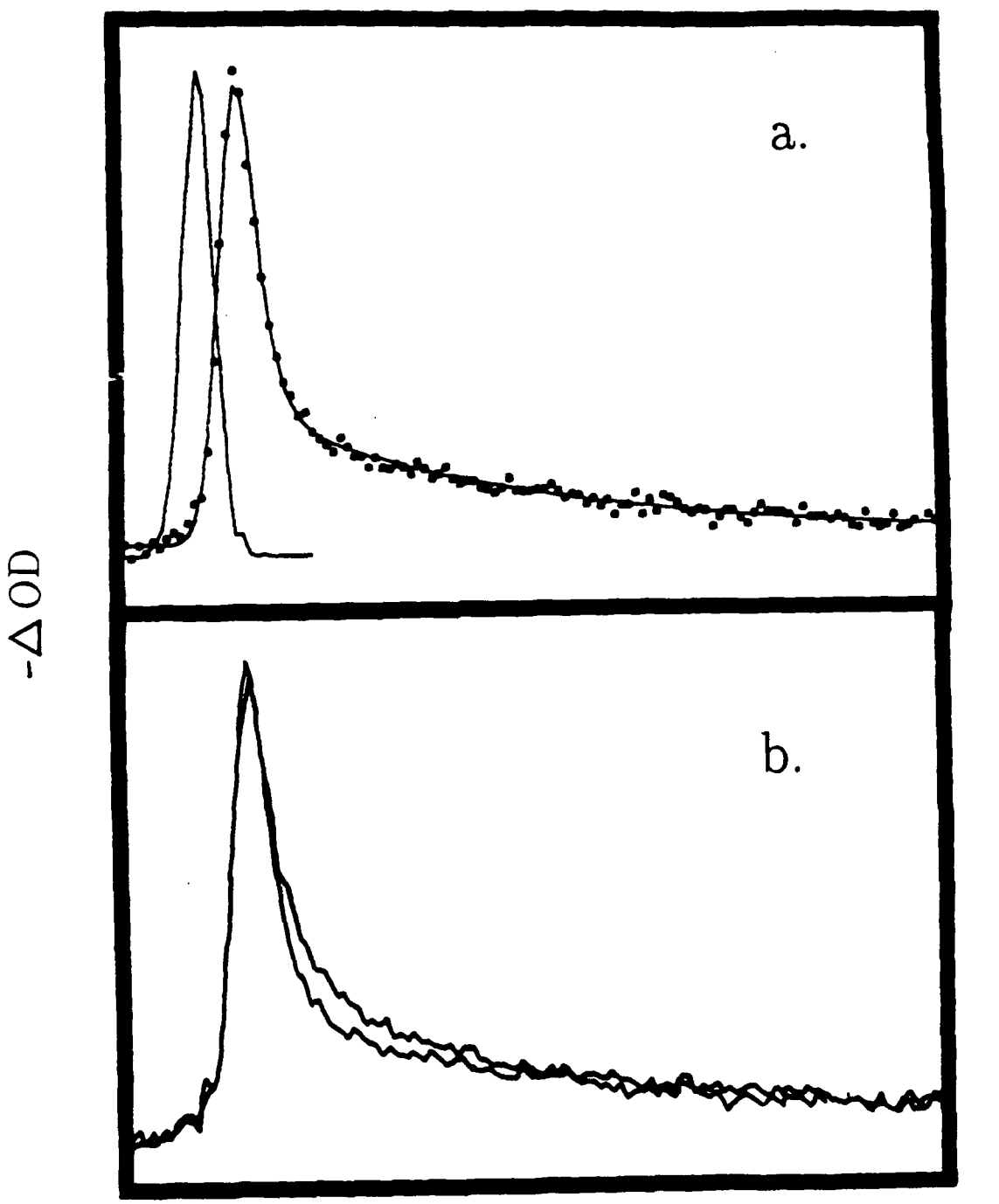

FIGURE 3

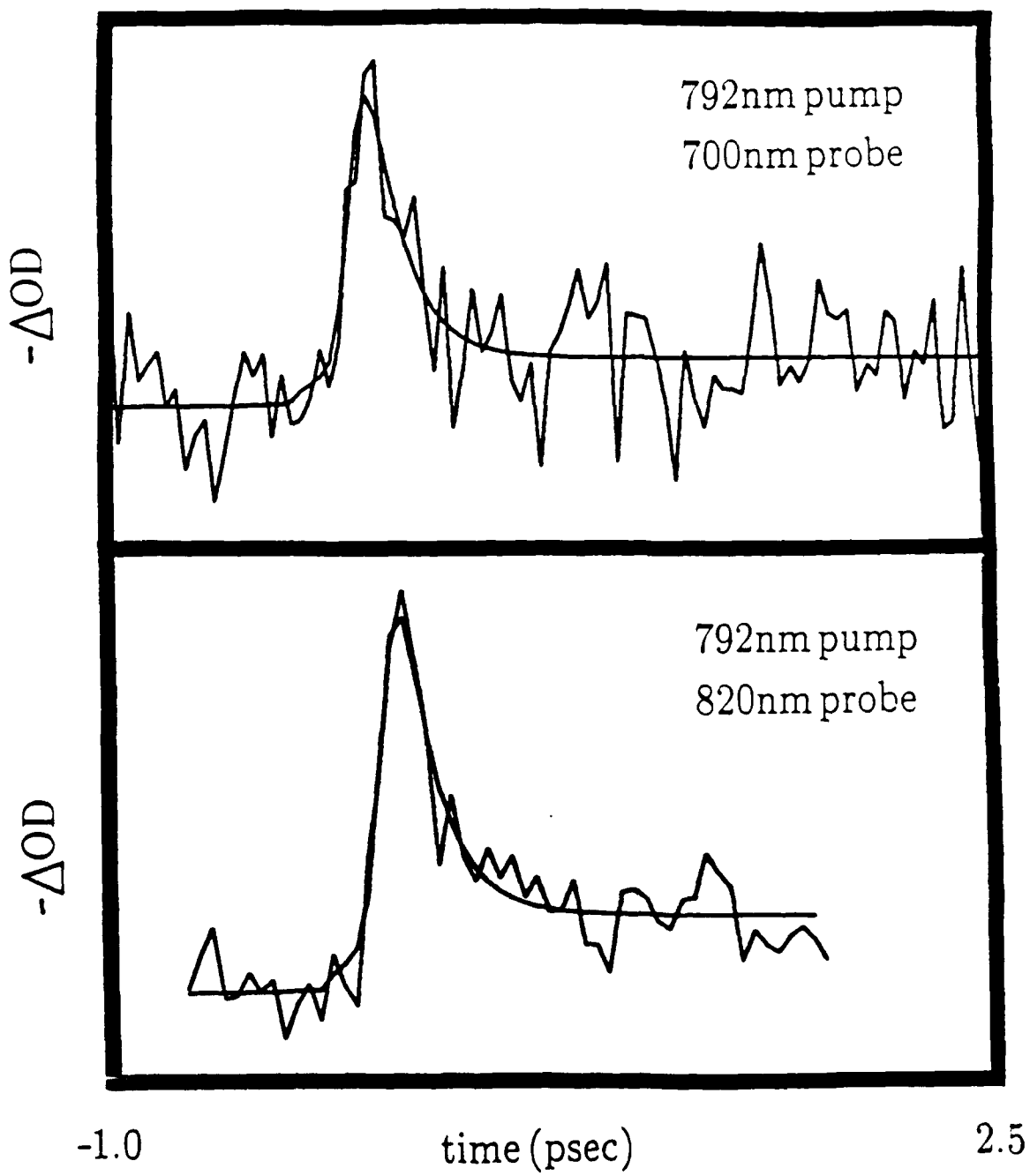
792nm pump
700nm probe
-ΔOD
792nm pump
820nm probe
-ΔOD
-1.0
time (psec)
2.5

TECHNICAL REPORT DISTRIBUTION LIST - GENERAL

Office of Naval Research (2)*
Chemistry Division, Code 1113
800 North Quincy Street
Arlington, Virginia 22217-5000

Dr. James S. Murday (1)
Chemistry Division, Code 6100
Naval Research Laboratory
Washington, D.C. 20375-5000

Dr. Robert Green, Director (1)
Chemistry Division, Code 385
Naval Weapons Center
China Lake, CA 93555-6001

Dr. Eugene C. Fischer (1)
Code 2840
David Taylor Research Center
Annapolis, MD 21402-5067

Dr. Elek Lindner (1)
Naval Ocean Systems Center
Code 52
San Diego, CA 92152-5000

Commanding Officer (1)
Naval Weapons Support Center
Dr. Bernard E. Douda
Crane, Indiana 47522-5050

Dr. Richard W. Drisko (1)
Naval Civil Engineering
Laboratory
Code L52
Port Hueneme, CA 93043

Dr. Harold H. Singerman (1)
David Taylor Research Center
Code 283
Annapolis, MD 21402-5067

Chief of Naval Research (1)
Special Assistant for Marine
Corps Matters
Code 00MC
800 North Quincy Street
Arlington, VA 22217-5000

Defense Technical Information
Center (2)
Building 5, Cameron Station
Alexandria, VA 22314

* Number of copies to forward

Enclosure (2)